Electronic Supplementary Material (ESI) for Materials Advances.

Electronic Supplementary Information for

Configuration dependent photovoltaic properties of cyclometalated heavy metal complexes for organic solar cells

Tianjian Yang, Aihua Zhou, Yinming He, Zhichao Yao, Xiaochen Song, Xianwang Tao, Youtian Tao*

Key Lab for Flexible Electronics and Institute of Advanced Materials, Nanjing Tech University, 30 South Puzhu Road, Nanjing, 211816, China

E-mail: iamyttao@njtech.edu.cn (Y. Tao)

Experomental Section

Materials and Synthesis:

All solvents were obtained commercially and used without further purification. Chlorobenzene and chloroform were purchased from Sigma Aldrich Co., $PC_{71}BM$ from One-Materials Inc. and Y6 from Nanjing Zhiyan Technology Co.. The tTBz-analogs based photovoltaic materials were synthesized according to Scheme S1 and the detailed synthetic procedures were outlined below.

Synthesis of tTBz:

2-(5-bromothiophen-2-yl)benzo[*d*]thiazole (500 mg, 1.72 mmol), 2-(5'-(tert-butyl)-[2,2'-bithiophen]-5-yl)-4,4,5,5-tetramethyl-1,3,2-dioxaborolane (705 mg, 2.03 mmol), K_2CO_3 (1.17 g, 8.41 mmol) and $Pd(PPh_3)_4$ (58.52 mg, 50.64 μmol) were stirred in the mixture solvent of toluene (25 mL), EtOH (2.5 mL) and H_2O (2.5 mL) refluxed at 110^{o}C for 24 h under a nitrogen atmosphere. After cooling to room temperature, the resulting mixture was extracted by CH_2Cl_2, then washed with brine, dried over anhydrous Na_2SO_4, and concentrated under reduced pressure. The crude product was purified by column chromatography using eluent with CH_2Cl_2:petroleum ether (1:1) and washed with MeOH to afford tTBz compound as yellow solid. (700 mg, 91%).

^{1}H NMR ($CDCl_3$, 400 MHz), δ (TMS, ppm): 8.00 (d, J = 8.1 Hz, 1H), 7.83 (d, J = 8.0 Hz, 1H), 7.53 (d, J = 3.9 Hz, 1H), 7.46 (t, J = 7.7 Hz, 1H), 7.35 (t, J = 7.4 Hz, 1H), 7.15 (dd, J = 8.8, 3.8 Hz, 2H), 7.01 (dd, J = 10.0, 3.7 Hz, 2H), 6.73 (d, J = 3.6 Hz, 1H), 1.39 (s, 9H). MALDI-TOF (m/z): M^+ calculated at 437.04, found at 436.93; Anal. Calcd for $C_{23}H_{19}NS_4$: C 63.12%, H 4.38%, N 3.20%, S 29.30%; found: C 62.86%, H 4.16%, N 3.25%, S 29.06%.

Synthesis of tTBzPt:

K_2PtCl_4 (200 mg, 482 μmol) and 2-(5''-(tert-butyl)-[2,2':5',2''-terthiophen]-5-yl)benzo[*d*]thiazole tTBz (253 mg, 578 μmol) were stirred in the mixture solvent of 2-ethoxyethanol (10 mL) and H_2O (3 mL) heated to 110^{o}C for 18h under a nitrogen atmosphere. After cooling the mixture to room temperature, it was added to water (5mL) and filtered the orange-yellow precipitate. The Pt dimer was washed by water and methanol in turn and used for the next step without any further purification. The Pt dimer (311 mg, 233.07 μmol), 2,2,6,6-tetramethylheptane-3,5-dione (84 mg, 465 μmol) and K_2CO_3 (160 mg, 1.24 mmol) were stirred in the solvent of 2-ethoxyethanol (15 mL) refluxed at 110°C for 18 h under a nitrogen atmosphere. After cooling to room temperature, the resulting mixture was extracted by CH_2Cl_2, then washed with brine, dried over anhydrous Na_2SO_4, and concentrated under reduced pressure. The crude product was purified by column chromatography using eluent with CH_2Cl_2: petroleum ether (1:1) and afford the title compound as orange to yellow solid tTBzPt (150 mg, 45%).

^1H NMR ($CDCl_3$, 400 MHz), δ (TMS, ppm): 9.13 (d, J = 8.3 Hz, 1H), 7.71 (d, J = 7.5 Hz, 1H), 7.46-7.50 (m, 1H), 7.31 (d, J = 21.4 Hz, 2H), 7.19 (t, J = 5.5 Hz, 1H), 7.02 (dd, J = 6.0, 3.7 Hz, 2H), 5.91 (s, 1H), 1.38 (s, 9H), 1.33 (s, 9H), 1.30 (s, 9H); MALDI-TOF (m/z): M^+ calculated at 814.14, found at 814.65; Anal. Calcd for $C_{34}H_{37}NO_2PtS_4$: C 50.11%, H 4.58%, N 1.72%, S 15.73%; found: C 50.23%, H 4.53%, N 1.71%, S 15.81%.

Synthesis of tTBzIr:

bis(2-(5-bromothiophen-2-yl)benzo[*d*]thiazole) iridium (pentane-2,4-dione) (200 mg, 227 μmol), 2-(5'-(tert-butyl)-[2,2'-bithiophen]-5-yl)-4,4,5,5-tetramethyl-1,3,2-dioxaborolane (174 mg, 499 μmol), K_2CO_3 (311 mg, 2.30 mmol) and $Pd(PPh_3)_4$ (15 mg, 12 μmol) were stirred in the mixture solvent of toluene (10 mL), EtOH (2 mL) and H_2O (4 mL) refluxed at 95°C for 24 h under a nitrogen atmosphere. After cooling to room temperature, the resulting mixture was extracted by CH_2Cl_2, then washed with brine, dried over anhydrous Na_2SO_4, and concentrated under reduced pressure. The crude product was purified by column chromatography using eluent with CH_2Cl_2: petroleum ether (1:1) and washed with MeOH to afford tTBzIr compound as red brown solid. (210 mg, 65%).

^1H NMR ($CDCl_3$, 400 MHz), δ (TMS, ppm): 7.88 (dd, J = 7.5，1.7 Hz, 2H), 7.81 (dd, J = 7.7，1.3 Hz, 2H), 7.34-7.39 (m, 4H), 6.93 (d, J = 3.8 Hz, 2H), 6.87 (dd, J = 3.7, 1.6 Hz, 4H), 6.65 (d, J = 3.7 Hz, 2H), 6.23 (s, 2H), 5.16 (s, 1H), 1.79 (s, 6H), 1.34 (s, 18H). MALDI-TOF (m/z): M^+ calculated at 1164.07, found at 1064.43; Anal. Calcd for $C_{51}H_{43}IrN_2O_2S_8$: C 52.60%, H 3.72%, N 2.41%, S 22.02%; found: C 52.80%, H 3.67%, N 2.43%, S 22.17%.

Synthesis of tTBz3Ir: The synthesis method of tTBz3Ir is the same as that of tTBzIr. tris(2-(5-bromothiophen-2-yl)benzo[*d*]thiazole) Ir (III) (200 mg, 185.56 μmol), 2-(5'-

(tert-butyl)-[2,2'-bithiophen]-5-yl)-4,4,5,5-tetramethyl-1,3,2-dioxaborolane (323.18 mg, 927.82 µmol), K_2CO_3 (384.69 mg, 2.78 mmol) and $Pd(PPh_3)_4$ (21.44 mg, 18.56 µmol). The crude product was purified by column chromatography using eluent with CH_2Cl_2: petroleum ether (1:2) and washed with MeOH to afford tTBz3Ir compound as red brown solid. (181 mg, 60%).

^1H NMR ($CDCl_3$, 400 MHz), δ (TMS, ppm): 7.71 (d, J = 8.0 Hz, 3H), 7.12 (t, J = 7.6 Hz, 3H), 7.07 (d, J = 3.8 Hz, 3H), 6.93 (t, J = 3.6 Hz, 6H), 6.88 (t, J = 7.2 Hz, 3H), 6.67 (d, J = 3.7 Hz, 3H), 6.61 (d, J = 8.2 Hz, 3H), 6.44 (s, 3H), 1.35 (s, 27H). MALDI-TOF (m/z): M^+ calculated at 1501.06, found at 1501.10; Anal. Calcd for $C_{69}H_{54}IrN_3S_{12}$: C 55.17%, H 3.62%, N 2.80%, S 25.61%; found: C 54.69%, H 3.51%, N 2.74%, S 25.28%.

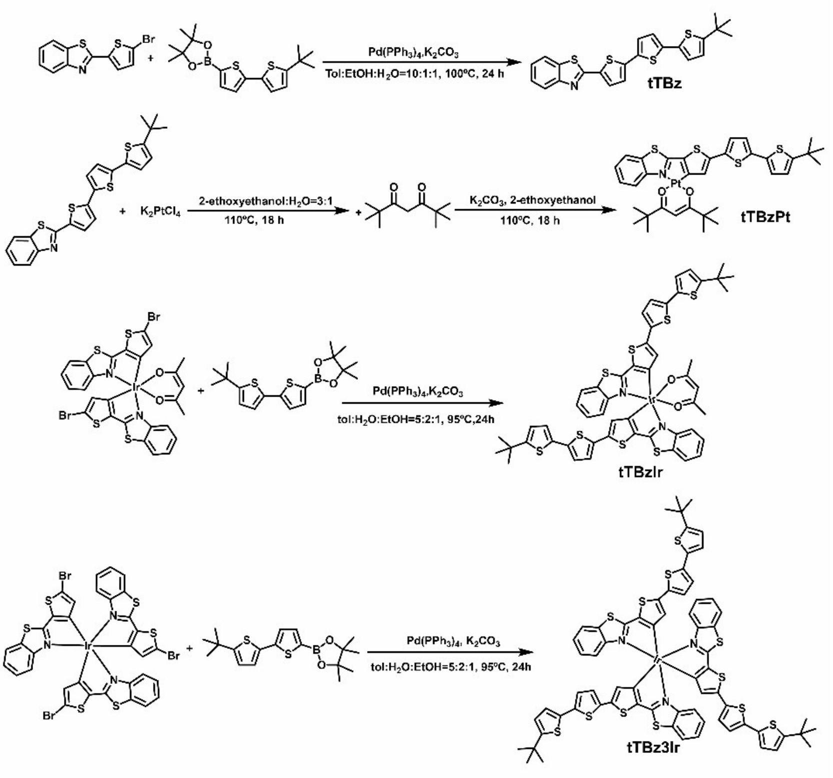

Scheme S1 Synthetic routes of tTBz, tTBzPt, tTBzIr and tTBz3Ir.

Measurement and characterization:

^1H NMR spectra were measured using a Bruker DMX-500 spectrometer in deuterochloroform with tetramethylsilane (TMS; δ=0 ppm) as an internal standard. Mass spectra were measured using a Bruker Autoflex matrix assisted laser desorption/ionization time-of-flight (MALDI-TOF). Elemental analysis (EA) of C, H, N and S were measured by a Vario EL Ⅲ micro analyzer. Ultraviolet-visible (UV-vis) absorption spectra of the thin films on a quartz substrate were measured using Shimadzu UV-2500 recording spectrophotometer. The photoluminescence (PL) spectra and transient lifetime were recorded using Edinburgh FLS-980 instrument. Thermal gravimetric analysis (TGA) was measured with a METTLER TOLEDO TGA2 instrument. The electrochemical cyclic voltammetry was conducted on a CHI voltammetric analyzer, in a 0.1 mol L^{-1} acetonitrile solution of tetrabutylammonium hexafluorophosphate (n-Bu_4NPF_6) at a potential scan rate of 100 mV s^{-1}. The conventional three electrode configuration consists of a platinum working electrode, a platinum wire counter electrode, and an Ag/AgCl wire pseudo-reference electrode. The sample was coated on the platinum sheet of working electrode. The reference electrode was checked versus ferrocenium-ferrocene (Fc^+/Fc) as internal standard as recommended by IUPAC (the vacuum energy level: -4.8 eV). All the solutions were deaerated by bubbling nitrogen gas for a few minutes prior to the electrochemical measurements. HOMO energy levels were calculated from the equation of $E_{\mathrm{HOMO}} = -(E_{\mathrm{onset}}(\mathrm{ox}) + 4.8)$ eV, and LUMO energy was deduced from the optical band gap (E_g) values and HOMO levels. *J-V* curves of OSCs devices were measured using a computer controlled Keithley 2400 Source Measure Unit under a simulated AM 1.5G spectrum, which was obtained by Oriel Sol3A Class Solar Simulator (model, Enlitech SS-F5-3A) with a 450 W xenon lamp and an air mass 1.5 filter. EQE spectra were measured by Solar Cell Spectral Response Measurement System QE-R3-011 (Enli Technology, Taiwan). Atom force microscopy (AFM) measurement was performed via Bruker Dimension ICON atomic force microscopy. Space-charge-limited-current (SCLC) electron and hole mobility were acquired through the electron- and hole-only devices with structures of ITO/ZnO/Active Layer/PDINO/Al and ITO/PEDOT:PSS/Active Layer/Au, respectively. The exciton dissociation probability $P_{(\mathrm{E,T})}$ was measured from the curves of photocurrent density (J_{ph}) versus effective voltage (V_{eff}). In detail, J_{ph} is defined as the difference between J_L and J_D, where J_L and J_D refer to the current density measured under one standard sun illumination and in the dark condition, respectively. V_{eff} can be calculated in the formula of $V_{\mathrm{eff}} = V_0 - V$, where V_0 is the voltage when $J_{\mathrm{ph}} = 0$, and V represents the applied voltage. As a result, the exciton dissociation probability ($P_{(\mathrm{E,T})}$) can be calculated according to the formula $P_{(\mathrm{E,T})} = J_{\mathrm{ph}}/J_{\mathrm{sat}}$, in which J_{sat} stands for the saturation photocurrent density. The charge recombination was detected through assessing the dependence of J_{sc} on the light intensity with a formula of $J_{\mathrm{sc}} \propto (P_{\mathrm{light}})^{\alpha}$, in which the exponential α stands for the degree of bimolecular recombination. Generally, when the α value is close to 1, it could be regarded that the bimolecular recombination in OSCs is negligible.

Fabrication of OSCs devices

OSCs with conventional structure of ITO/PEDOT:PSS/active layer/PDINO/Al were fabricated as follows. Indium tin oxide (ITO) glass substrates were cleaned in an ultrasonic bath with detergent, deionized water, acetone and isopropanol, respectively, and followed by treatment of UV-ozone for 30 minutes. Then, PEDOT:PSS (Baytron PVP Al 4083) was spin-coated on the ITO at 3500 rpm for 60 seconds and baked at 150°C for 15 min in air to give a film thickness around 30 nm. After that, the substrates with PEDOT:PSS thin film were transferred to a nitrogen glove box. For PCBM system, the tTBz:PCBM (1:1, w/w), tTBzPt:PCBM (1:2.5, w/w), tTBzIr:PCBM (1:1, w/w) and tTBz3Ir:PCBM (0.7:1, w/w) mixed CB solution with total concentration of 20, 15, 20 and 20 mg mL^{-1} were spin-coated at 2000 rpm in the nitrogen glove box. And for the devices based on Y6, all of the blend films were dissolved in $CHCl_3$ solvent (D:A = 1:1, w/w, 20 mg mL^{-1}) anteriorly with stirring over 12 hours under 60°C, and then spin-coated at 2000 rpm. A cathode buffer layer PDINO was then spin-coated at 3000 rpm for 60 seconds. Finally, aluminum with a thickness of 100 nm was evaporated onto the PDINO layer under vacuum ($\approx 10^{-5}$ Pa) as the back electrode. The devices based on TBz and TBzIr were fabricated according to our previous report.

Additional Figures and Tables

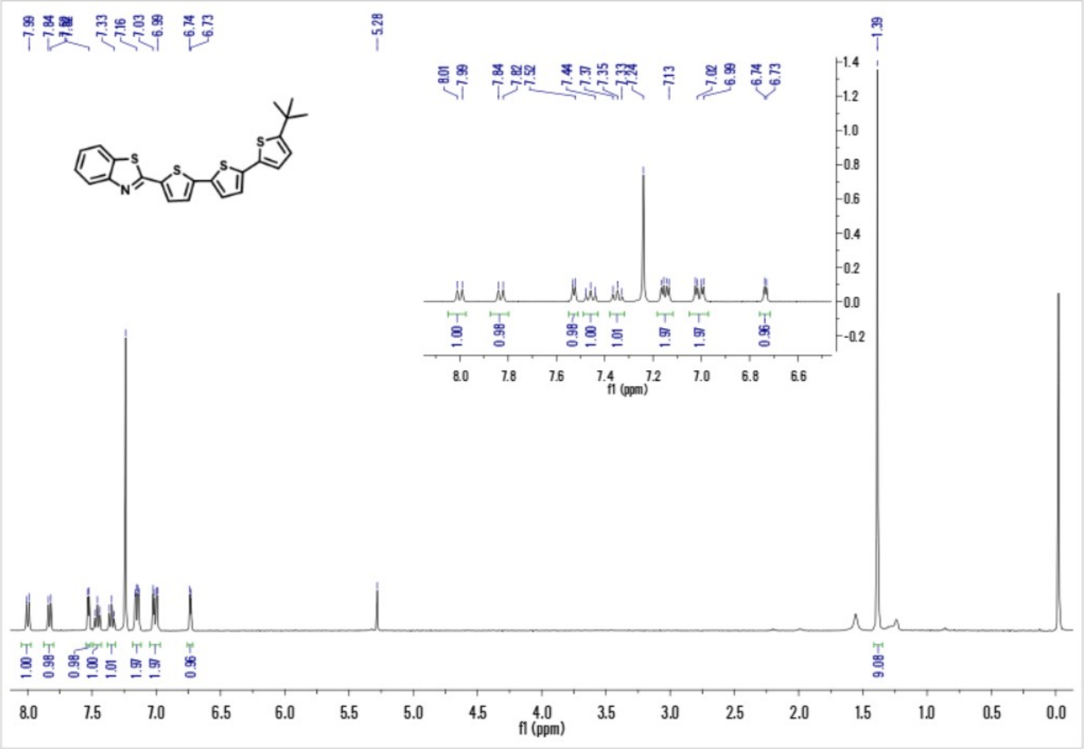

Fig. S1 ^{1}H NMR spectrum of tTBz.

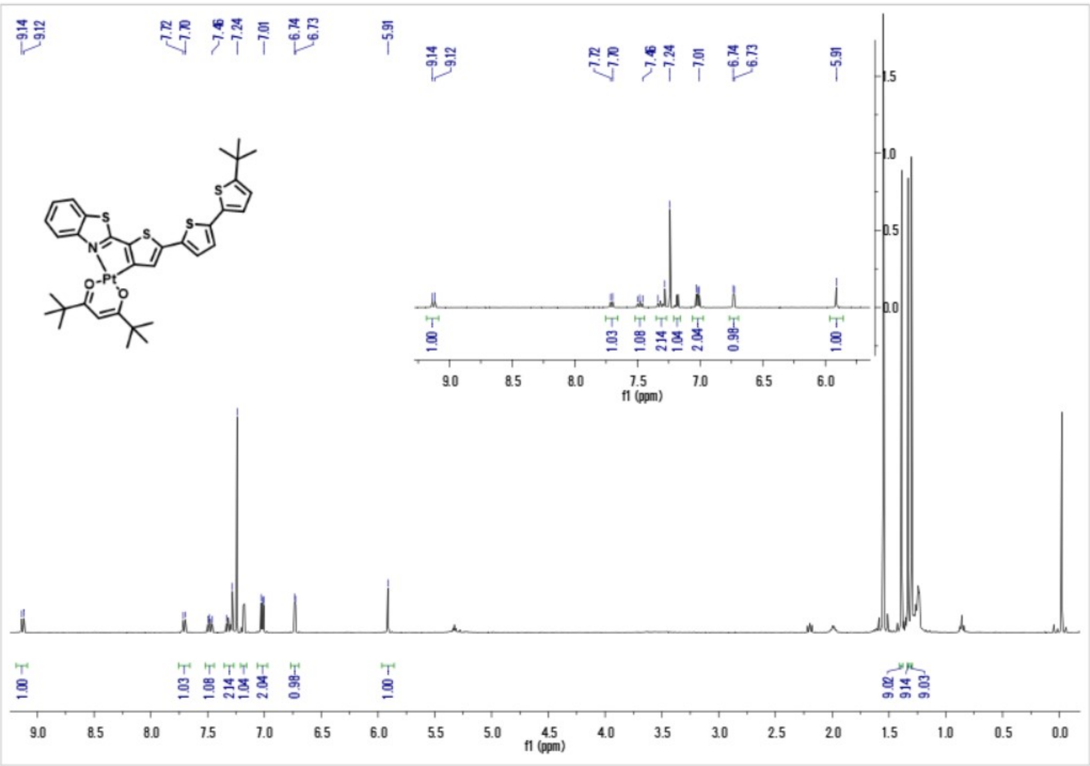

Fig. S2 ^{1}H NMR spectrum of tTBzPt.

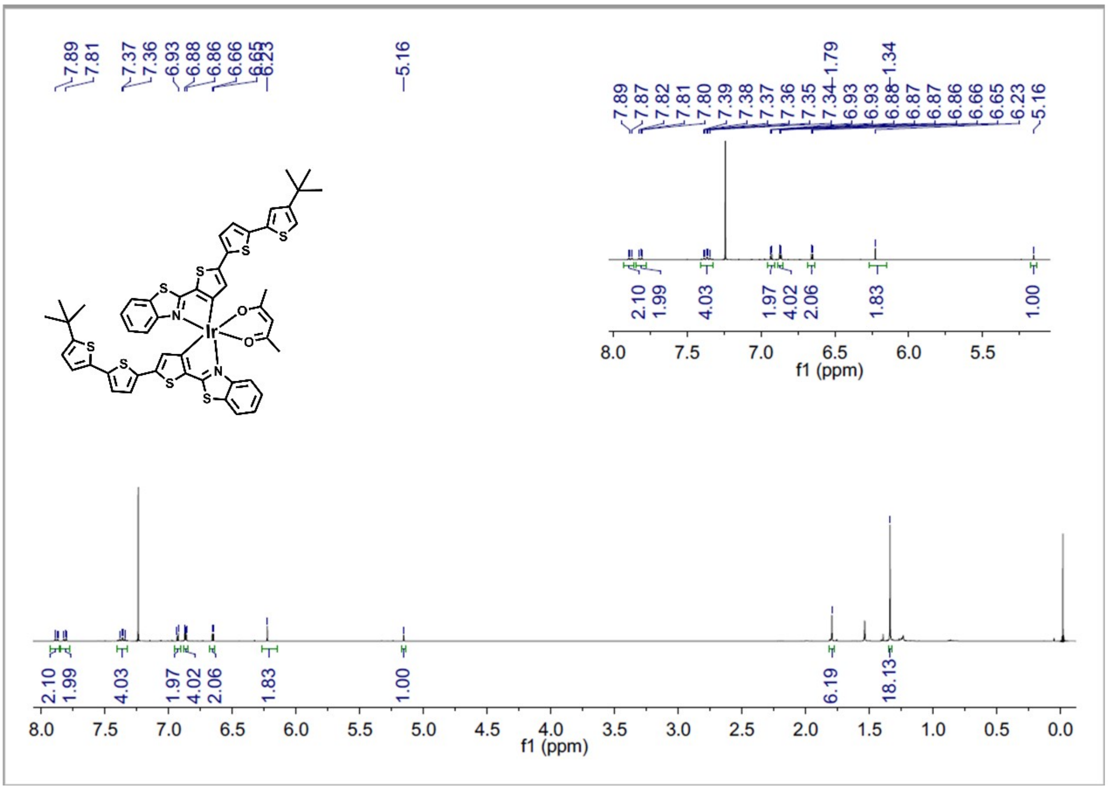

Fig. S3 ^{1}H NMR spectrum of tTBzIr.

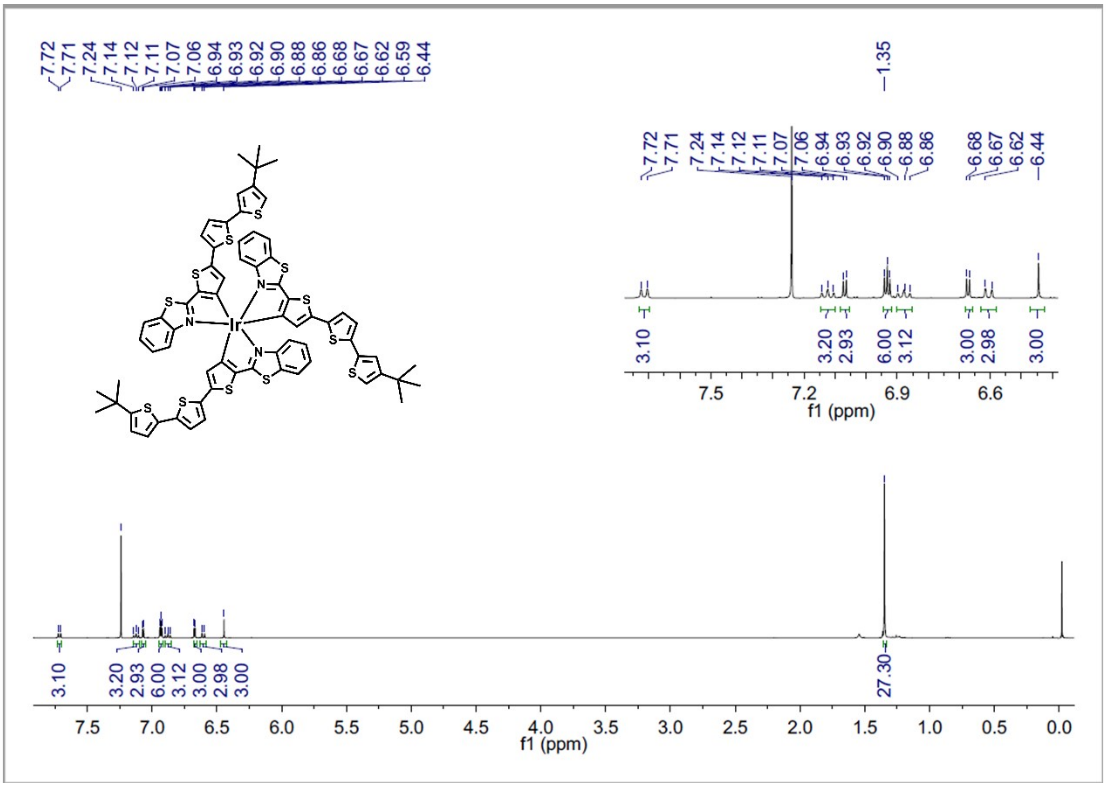

Fig. S4 ^{1}H NMR spectrum of tTBz3Ir.

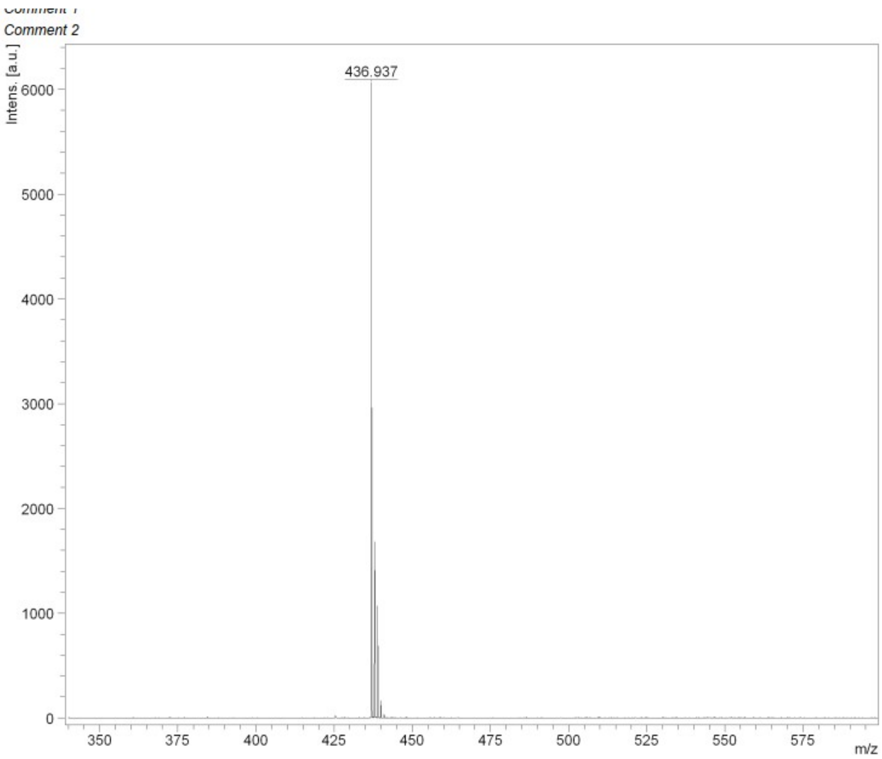

Fig. S5 The mass spectrometry of tTBz.

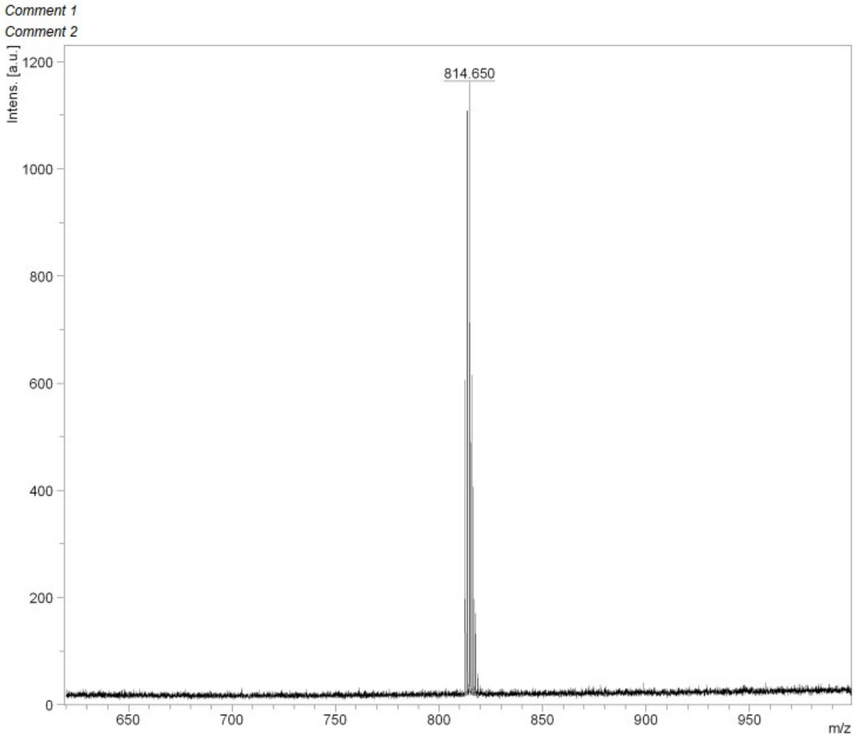

Fig. S6 The mass spectrometry of tTBzPt.

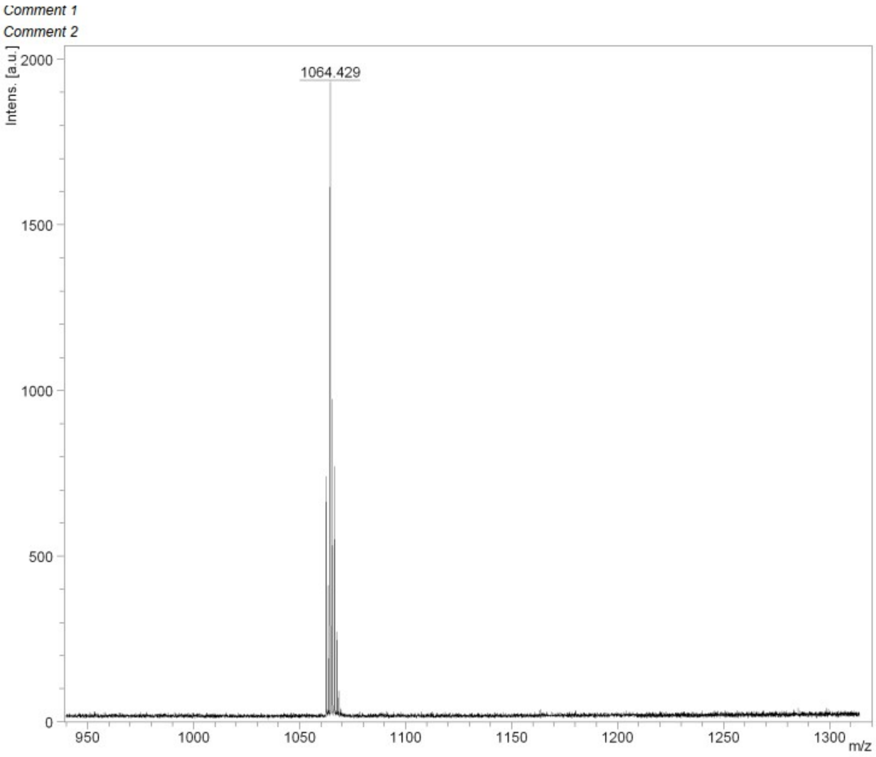

Fig. S7 The mass spectrometry of tTBzIr.

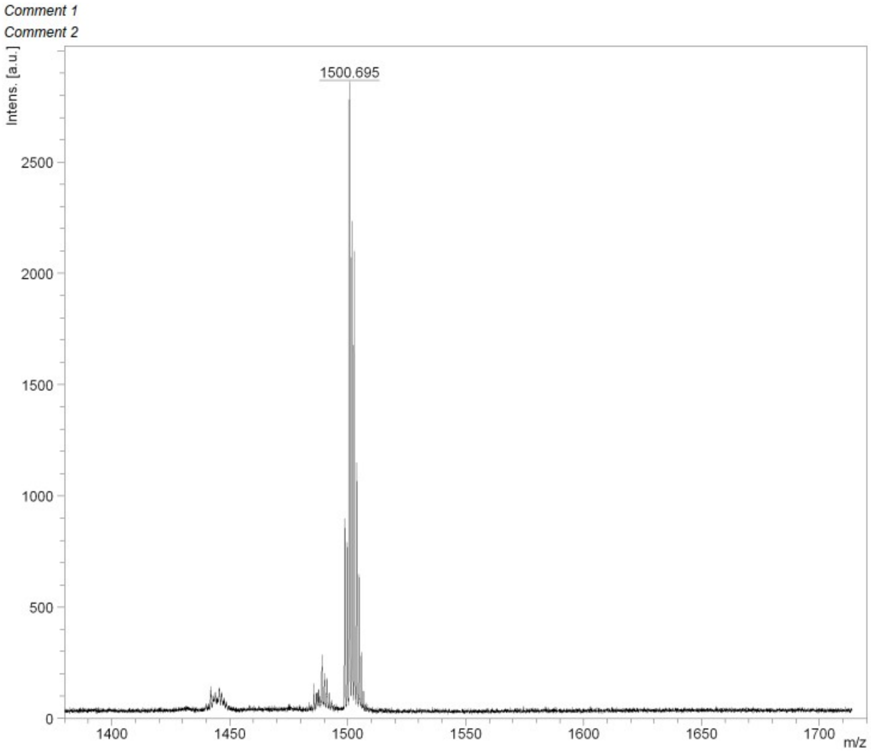

Fig. S8 The mass spectrometry of tTBz3Ir.

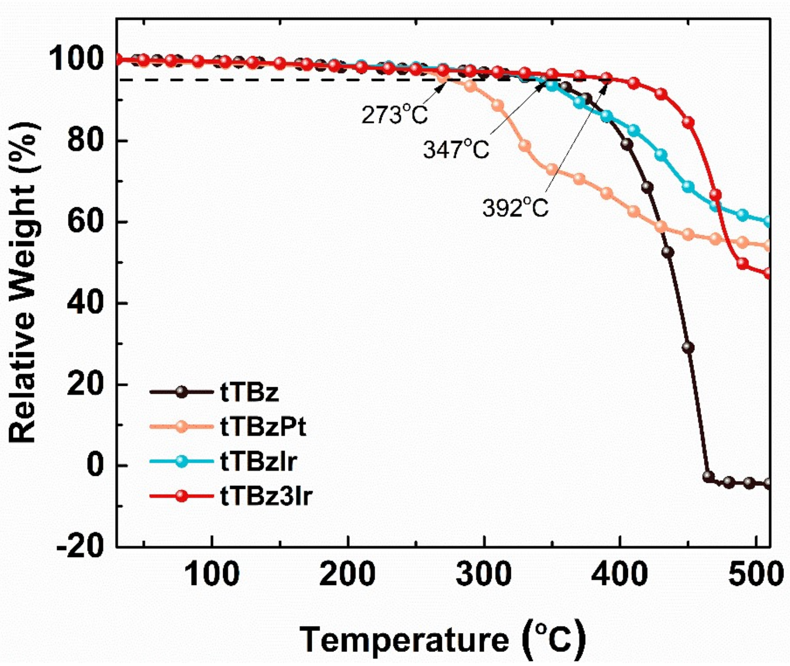

Fig. S9 The TGA curves for tTBz, tTBzPt, tTBzIr and tTBz3Ir.

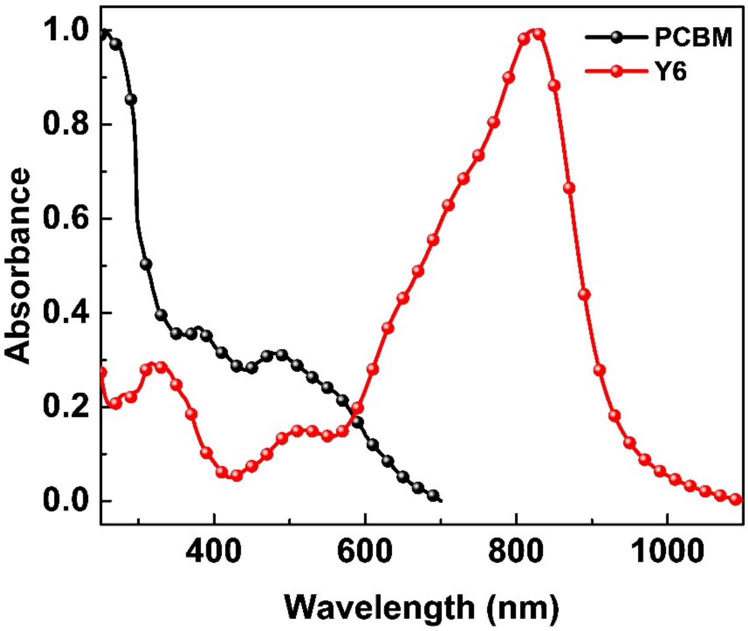

Fig. S10 The normalized UV-Vis absorption spectra of acceptor materials in film state.

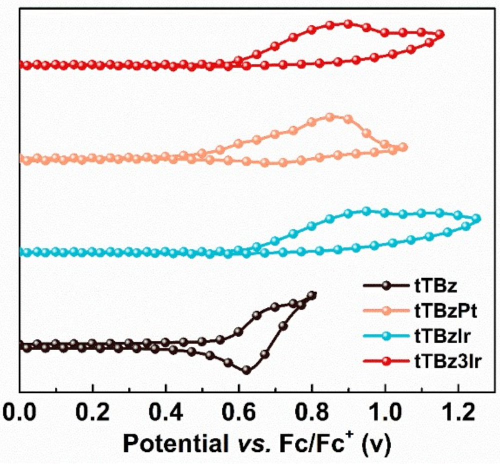

Fig. S11 The cyclic voltammograms of tTBz, tTBzPt, tTBzIr and tTBz3Ir.

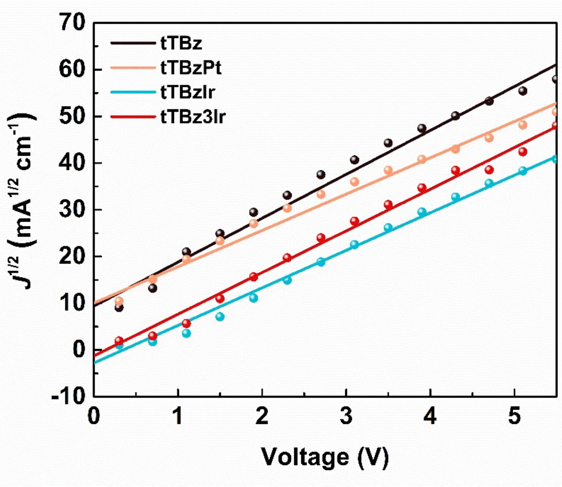

Fig. S12 $J^{1/2}$-V plots of hole-only devices based on tTBz, tTBzPt, tTBzIr and tTBz3Ir.

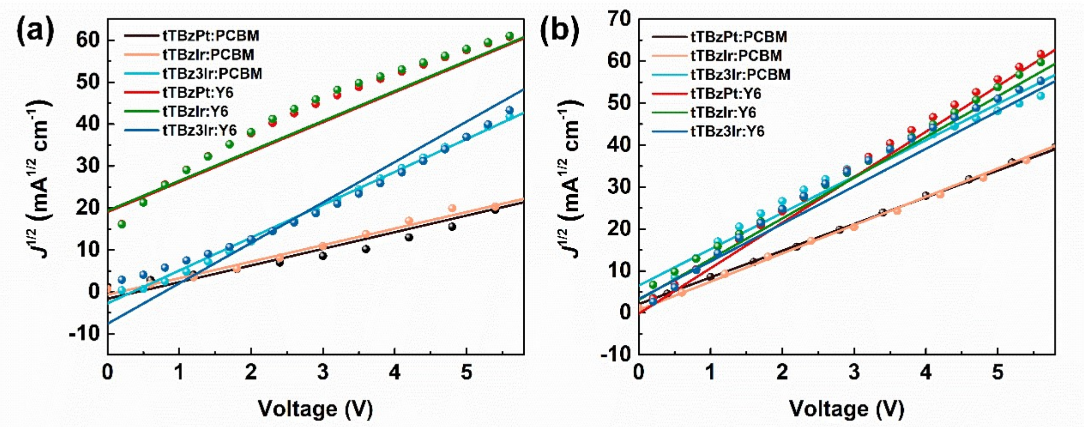

Fig. S13 $J^{1/2}$-V plots of (a) hole-only and (b) electron-only devices based on corresponding blended films.

Table S1 Photovoltaic parameters of OSCs based on tTBzPt:PCBM with different D:A weight ratio.

tTBzPt:PCBM	V_{oc} (V)	J_{sc} (mA cm^{-2})	FF	PCE (%)
1.5:1	0.68	1.36	0.25	0.23 (0.21±0.02)
1:0.8	0.68	1.56	0.25	0.28 (0.26±0.02)
1:1	0.71	1.76	0.27	0.33 (0.32±0.01)
0.8:1	0.74	2.14	0.26	0.42 (0.40±0.02)
1:1.5	0.80	2.55	0.26	0.54 (0.48±0.06)
1:2	0.83	3.84	0.26	0.83 (0.76±0.07)
1:2.5	0.80	3.99	0.27	0.88 (0.84±0.04)
1:3	0.71	3.90	0.27	0.07 (0.64±0.06)

Table S2 Photovoltaic parameters of OSCs based on tTBzPt:PCBM with different thickness of active layers.

tTBzPt:PCBM	V_{oc} (V)	J_{sc} (mA cm^{-2})	FF	PCE (%)
71.4 nm	0.83	3.32	0.29	0.79 (0.74±0.05)
81.1 nm	0.83	3.53	0.28	0.81 (0.77±0.04)
89.2 nm	0.86	4.18	0.28	0.96 (0.88±0.08)
94.7 nm	0.83	3.82	0.28	0.83 (0.82±0.01)
104.8 nm	0.80	3.58	0.27	0.74 (0.73±0.01)

Table S3 Photovoltaic parameters of OSCs based on tTBzIr:PCBM with different D:A weight ratio.

tTBzIr:PCBM	V_{oc} (V)	J_{sc} (mA cm^{-2})	FF	PCE (%)
1.5:1	0.92	6.49	0.36	2.01 (1.97±0.04)
1:0.8	0.92	8.39	0.43	3.15 (3.06±0.09)
1:1	0.92	8.65	0.47	3.75 (3.66±0.09)
0.8:1	0.89	8.55	0.50	3.61 (3.43±0.18)
1:1.5	0.89	7.98	0.49	3.21 (3.13±0.08)

Table S4 Photovoltaic parameters of OSCs based on tTBzIr:PCBM with different thickness of active layers.

tTBzIr:PCBM	V_{oc} (V)	J_{sc} (mA cm^{-2})	FF	PCE (%)
70.3 nm	0.89	7.77	0.44	2.87 (2.74±0.10)
82.5 nm	0.89	7.98	0.43	3.00 (2.79±0.21)
90.8 nm	0.92	8.98	0.46	3.71 (3.45±0.26)
110.1 nm	0.92	9.30	0.43	3.56 (3.37±0.19)
152.4 nm	0.92	8.10	0.41	3.06 (2.85±0.21)

Table S5 Photovoltaic parameters of OSCs based on tTBz3Ir:PCBM with different D:A weight ratio.

tTBz3Ir:PCBM	V_{oc} (V)	J_{sc} (mA cm^{-2})	FF	PCE (%)
1.5:1	0.99	7.34	0.37	2.68 (2.61±0.07)
1:0.8	0.96	8.39	0.45	3.63 (3.46±0.17)
1:1	0.96	9.10	0.48	4.00 (3.79±0.21)
0.9:1	0.96	10.11	0.51	5.01 (4.78±0.23)
0.8:1	0.96	10.72	0.54	5.32 (5.16±0.17)
0.7:1	0.96	10.91	0.55	5.71 (5.44±0.27)
0.6:1	0.96	10.31	0.54	5.26 (5.04±0.22)
0.5:1	0.96	9.69	0.54	4.96 (4.69±0.27)

Table S6 Photovoltaic parameters of OSCs based on tTBz3Ir:PCBM with different thickness of active layers.

tTBz3Ir:PCBM	V_{oc} (V)	J_{sc} (mA cm^{-2})	FF	PCE (%)
84.0 nm	0.96	8.31	0.57	4.51 (4.28±0.23)
95.1 nm	0.96	9.24	0.57	4.69 (4.60±0.09)
101.2 nm	0.96	9.21	0.55	4.74 (4.38±0.36)
111.3 nm	0.96	9.95	0.56	5.07 (4.93±0.14)
118.6 nm	0.96	10.53	0.55	5.18 (5.02±0.16)
130.1 nm	0.96	10.17	0.54	5.00 (4.62±0.38)